Development and Characterization of Clinical-Grade ^{89}Zr-Trastuzumab for HER2/*neu* ImmunoPET Imaging

Eli C.F. Dijkers[1,2], Jos G.W. Kosterink[1], Anna P. Rademaker[1], Lars R. Perk[3], Guus A.M.S. van Dongen[3], Joost Bart[4], Johan R. de Jong[2], Elisabeth G.E. de Vries[5], and Marjolijn N. Lub-de Hooge[1,2]

[1]*Department of Hospital and Clinical Pharmacy, University Medical Center Groningen, University of Groningen, Groningen, The Netherlands;* [2]*Department of Nuclear Medicine and Molecular Imaging, University Medical Center Groningen, University of Groningen, Groningen, The Netherlands;* [3]*Department of Otolaryngology/Head and Neck Surgery, VU University Medical Center, Amsterdam, The Netherlands;* [4]*Department of Pathology, University Medical Center Groningen, University of Groningen, Groningen, The Netherlands; and* [5]*Department of Medical Oncology, University Medical Center Groningen, University of Groningen, Groningen, The Netherlands*

The anti–human epidermal growth factor receptor 2 (HER2/*neu*) antibody trastuzumab is administered to patients with HER2/*neu*-overexpressing breast cancer. Whole-body noninvasive HER2/*neu* scintigraphy could help to assess and quantify the HER2/*neu* expression of all lesions, including nonaccessible metastases. The aims of this study were to develop clinical-grade radiolabeled trastuzumab for clinical HER2/*neu* immunoPET scintigraphy, to improve diagnostic imaging, to guide antibody-based therapy, and to support early antibody development. The PET radiopharmaceutical ^{89}Zr-trastuzumab was compared with the SPECT tracer ^{111}In-trastuzumab, which we have tested in the clinic already. **Methods:** Trastuzumab was labeled with ^{89}Zr and (for comparison) with ^{111}In. The minimal dose of trastuzumab required for optimal small-animal PET imaging and biodistribution was determined with human HER2/*neu*-positive or -negative tumor xenograft–bearing mice. **Results:** Trastuzumab was efficiently radiolabeled with ^{89}Zr at a high radiochemical purity and specific activity. The antigen-binding capacity was preserved, and the radiopharmaceutical proved to be stable for up to 7 d in solvent and human serum. Of the tested protein doses, the minimal dose of trastuzumab (100 μg) proved to be optimal for imaging. The comparative biodistribution study showed a higher level of ^{89}Zr-trastuzumab in HER2/*neu*-positive tumors than in HER2/*neu*-negative tumors, especially at day 6 (33.4 ± 7.6 [mean ± SEM] vs. 7.1 ± 0.7 percentage injected dose per gram of tissue). There were good correlations between the small-animal PET images and the biodistribution data and between ^{89}Zr-trastuzumab and ^{111}In-trastuzumab uptake in tumors (R^2 = 0.972). **Conclusion:** Clinical-grade ^{89}Zr-trastuzumab showed high and HER2/*neu*-specific tumor uptake at a good resolution.

Key Words: HER2/*neu*; immunoPET; imaging; breast cancer

Human epidermal growth factor receptor 2 (HER2/*neu*) belongs to the ErbB tyrosine kinase receptor family, which consists of 4 receptors, HER1–HER4. Members of the HER family have growth-stimulating activity and play an important role in the regulation of cell growth, survival, and differentiation (*1*). HER2/*neu* is genetically encoded by the HER2/*neu* proto-oncogene (HER2/*neu* or c-erbB-2). HER2/*neu* overexpression or amplification occurs in a wide range of human cancers, including breast (incidence, 20%−30%), colon, lung, and ovarian cancers (*2,3*). HER2/*neu* overexpression and amplification are associated with oncogenic transformation and, for breast cancer, with a poorer prognosis and more aggressive behavior of the tumor in the clinical setting when no HER2/*neu*-directed therapy is used (*4–8*). HER2/*neu* is therefore a relevant target for therapy in breast cancer in the metastatic setting as well as in the adjuvant setting (*9*). The monoclonal antibody (mAb) trastuzumab and the dual-target (epidermal growth factor receptor 1 and HER2/*neu* tyrosine kinase) inhibitor lapatinib are currently used in clinical practice to target HER2/*neu*.

To determine HER2/*neu* overexpression or amplification in tumor biopsies, a wide variety of techniques have been used. Of these, immunohistochemistry and fluorescence in situ hybridization are currently the standard techniques (*10,11*).

Although the HER2/*neu* status provides important information about the molecular composition of the tumor, it is generally only determined at diagnosis of the primary tumor. The HER2/*neu* tumor status can show a time-dependent change after therapy and can be different across tumor lesions in a single patient (*12*). Repeat biopsies would be an interesting way to analyze the HER2/*neu* tumor status during the course of the disease because of the possible time-dependent change in status after therapy. However, doctors and patients are frequently reluctant to use invasive techniques,

particularly for poorly accessible lesions (13). Whole-body noninvasive HER2/*neu* scintigraphy could be a strategy for determining the HER2/*neu* expression of all lesions, including nonaccessible distant metastases, in a single scan and overcoming this problem. In addition, immunoscintigraphy could help to improve diagnostic imaging and to guide antibody-based therapy.

This situation has led to the development of ^{111}In-radiolabeled trastuzumab. Using SPECT, we have shown HER2/*neu*-specific uptake of this radiopharmaceutical in xenograft-bearing animals (14) and HER2/*neu*-positive metastatic breast cancer patients (15). ^{111}In-diethylamine-triaminepentaacetic acid (DTPA)-trastuzumab scintigraphy revealed new tumor lesions in 13 of 15 patients and was therefore considered to be of potential value for clinical staging (15).

In an attempt to further optimize HER2/*neu* imaging, PET was used instead of conventional nuclear medicine techniques because of its higher spatial resolution, better signal-to-noise ratio, and straightforward data quantification.

In line with our previous studies, our goal was to develop a radiopharmaceutical suitable for clinical HER2/*neu* immunoPET scintigraphy. The new PET radiopharmaceutical had to be at least comparable to ^{111}In-DTPA-trastuzumab in uptake, biodistribution, and imaging quality. Here we describe the development and in vitro and in vivo characterization of [89]Zr-radiolabeled trastuzumab and a comparison of [89]Zr-trastuzumab with ^{111}In-trastuzumab.

MATERIALS AND METHODS

The trastuzumab conjugation and labeling procedures described here were performed under good manufacturing practice (GMP) conditions at our manufacturing licensed department of nuclear medicine and molecular imaging. Materials and solvents for the labeling procedure were sterile and endotoxin and metal free (except for the Vivaspin-2 filters [see next paragraph]). Protein concentration, endotoxin content, and sterility were measured. Both radiopharmaceuticals met European Pharmacopoeia and U.S. Pharmacopoeia requirements for sterile radiopharmaceuticals. All chemicals used for the study complied with European Pharmacopoeia or U.S. Pharmacopoeia specifications.

[89]Zr-Trastuzumab Production

In the first step, reconstituted trastuzumab (21 mg/mL; Roche) was purified with water for injection from excipients by ultrafiltration. Vivaspin-2 filters (30 kDa; Sartorius AG; 2×10 min at $2,684g$) were used for all ultrafiltration purification steps. Purified trastuzumab was conjugated essentially as described by Verel et al. (16). In short, trastuzumab was diluted with 0.1 M Na_2CO_3 (pH 9.5; Bufa) and allowed to react with a 2-fold molar excess of a tetrafluorophenol-*N*-succinyldesferal-Fe (TFP-*N*-SucDf-Fe; VU University Medical Center) active ester. After 30 min, the pH was adjusted to 4.0 with sulfuric acid (Merck). The number of desferal ligands per antibody was assessed by size exclusion high-performance liquid chromatography (SE-HPLC) at 430 nm, and ethylenediaminetetraacetic acid (Merck) was added to remove Fe(III). The premodified antibody was purified by ultrafiltration with 0.9% sterile NaCl (B. Braun) and immediately used or stored

at $-80°C$. Frozen *N*-SucDf-trastuzumab proved to be stable for at least 12 mo. In the second step, the conjugate was radiolabeled with clinical-grade [89]Zr-oxalate (99.99% pure; BV Cyclotron, VU University Medical Center) in 1 M *N*-2-hydroxyethylpiperazine-*N′*-2-ethanesulfonic acid (HEPES, pH 6.8; Invitrogen) and purified by ultrafiltration with 0.9% NaCl:0.5% gentisic acid (Merck) to obtain a radiochemical purity of at least 95%. [89]Zr-*N*-SucDf-trastuzumab is hereafter referred to as [89]Zr-trastuzumab.

[111]In-Trastuzumab Production

Conjugation and radiolabeling were performed as described by Ruegg et al. (17). First, purified trastuzumab was conjugated in 0.1 M $NaHCO_3$ (pH 8.4; Merck) with a 25-fold molar excess of the bifunctional chelate 2-(4-isothiocyanatobenzyl)-DTPA (*p*-SCN-Bn-DTPA; Macrocyclics). Unbound conjugate was removed by ultrafiltration with 0.15 M acetate buffer (pH 5.5, freshly prepared from ammonia and acetic acid, both obtained from Merck). The conjugated antibody was immediately used or stored at $-80°C$. Frozen *p*-SCN-Bn-DTPA-trastuzumab proved to be stable for at least 12 mo. Conjugated trastuzumab was radiolabeled with [111]$InCl_3$ (370 MBq/mL, >1.85 GBq/mg, 99.9% radionuclidic purity; Covidien) in 0.15 M acetate buffer (pH 5.5), and the number of DTPA ligands per trastuzumab molecule was established as described by Hnatowich et al. (18). To obtain a radiochemical purity of at least 95%, we purified [111]In-*p*-SCN-Bn-DTPA-trastuzumab by ultrafiltration with 0.15 M acetate buffer. [111]In-*p*-SCN-Bn-DTPA-trastuzumab is hereafter referred to as ^{111}In-trastuzumab.

Quality Control of Premodified and Radiolabeled Trastuzumab

Radiochemical purity and stability were confirmed by SE-HPLC and by 30% trichloroacetic acid (TCA; Department of Hospital and Clinical Pharmacy, University Medical Center Groningen [UMCG]) precipitation for [89]Zr-trastuzumab or thin-layer chromatography (TLC) for ^{111}In-trastuzumab.

The Waters SE-HPLC system was equipped with a dual-wavelength absorbance detector, an in-line radioactivity detector, and a size exclusion column (Superdex 200 10/300 GL; GE Healthcare). Sodium phosphate buffer (0.025 M $Na_2HPO_4·2H_2O$ and $NaH_2PO_4·H_2O$, both obtained from Sigma-Aldrich) was used as a mobile phase. The retention time for trastuzumab was approximately 17 min; [89]Zr-*N*-SucDf, ^{111}In-DTPA, and low-molecular-weight impurities eluted at 28 min (at a flow of 0.7 mL/min).

TCA precipitation was performed with phosphate-buffered saline, 0.5% human serum albumin (Sanquin), and 30% TCA. Radioactivity was determined with a calibrated well-type γ-counter (LKB 1282; Compugamma).

TLC was performed with silica-impregnated glass fiber sheets (TLC-SG, 2.5×10 cm; Pall Gelman Sciences), and 0.1 M citrate buffer (pH 6.0) was used for elution. Radioactivity was determined with an instant chromatography scanner (VCS-IOI; Veenstra Instruments) equipped with an NaI crystal.

Immunoreactive Fraction

Flow cytometry was performed with trastuzumab and a fluorescein isothiocyanate–labeled antihuman antibody (F5016; Sigma-Aldrich) to confirm HER2/*neu* expression as described earlier (19). The in vitro binding characteristics (immunoreactive fraction) of radiolabeled trastuzumab were determined in a cell-binding assay, essentially as described by Lindmo et al. (20), with SKOV3 (a naturally HER2/*neu*-overexpressing human ovarian cancer cell line) and GLC4 (a HER2/*neu*-negative human small cell lung cancer cell line).

SKOV3 cells were cultured in Dulbecco's modified Eagle's medium with a high glucose concentration, and GLC4 cells were cultured in RPMI 1640 medium, both with 10% fetal calf serum. SKOV3 cells were harvested with trypsin; GLC4 cells grow in suspension.

For the antigen-binding experiment, cells were collected, and a fixed amount of radioactivity (10,000 cpm) was added to an increasing number of cells. After 1 h of incubation, the cell suspensions were centrifuged and repeatedly washed with phosphate-buffered saline containing 0.5% human serum albumin to determine the radioactivity uptake. The specific binding was calculated as the ratio of cell-bound radioactivity to the total amount of applied radioactivity and was corrected for nonspecific binding, as determined with a 500-fold excess of nonradioactive trastuzumab. All binding assays were performed in triplicate.

Stability Testing of Radiolabeled Compounds

The stability of the labeled compounds was evaluated at 4°C in solution (0.9% NaCl:0.5% gentisic acid or ammonium acetate [pH 5.5] for ^{89}Zr-trastuzumab and ^{111}In-trastuzumab, respectively) and in human serum at 37°C for 7 d. The radiochemical purity and the immunoreactive fraction were determined by SE-HPLC, TLC, or TCA precipitation and the assay described by Lindmo et al. (20).

In Vivo Biodistribution Studies

An animal study was conducted to assess the minimal dose of trastuzumab required for optimal imaging, to determine HER2/*neu*-specific tumor uptake, and to compare ^{89}Zr-trastuzumab and ^{111}In-trastuzumab biodistributions in mice bearing human ovarian carcinoma SKOV3 (HER2/*neu*-positive) or human small cell lung carcinoma GLC4 (HER2/*neu*-negative) xenografts. Male athymic mice (Hsd:Athymic Nude/*nu*) were obtained from Harlan. All animal studies were conducted in accordance with the Dutch Law on Animal Experimentation and were approved by the local ethics committee. At 4–6 wk of age (weight, 30 g), the mice were injected subcutaneously with 10^6 tumor cells (mixed with equal amounts of Matrigel [Becton Dickinson]). Approximately 2 wk after inoculation, animals were used for the in vivo studies (tumor diameters, 5–8 mm).

Protein Dose Escalation Study

Before a larger biodistribution study was carried out, a protein dose escalation study was performed to determine the minimal dose of trastuzumab required for optimal imaging. SKOV3 xenograft–bearing nude mice (5 per group) were injected intravenously in the penile vein with 5 MBq of ^{89}Zr-trastuzumab, corresponding to a total amount of 100, 250, or 500 μg of trastuzumab per animal. At 1, 3, and 6 d after injection, animals were anesthetized with 2% isoflurane and underwent small-animal PET imaging (Focus 220 microPET scanner; Siemens) in the transaxial position for 30–60 min. A transmission scan with a ^{57}Co point source was used for scatter and attenuation corrections. Images were reconstructed in the 2-dimensional ordered-subset expectation maximization mode with 4 iterations by use of microPET manager (Siemens). The voxel size of the images was $0.47 \times 0.47 \times 0.82$ mm, and a gaussian filter of 1.2 mm was applied to the images after reconstruction.

In vivo quantification was performed with AMIDE Medical Image Data Examiner software (version 0.9.1; Stanford University) (21).

The accumulation of radioactivity in tumors and a representative subset of the tumor volume were determined by drawing an 80% isodensity contour volume of interest around the tumor on the small-animal PET images as previously described (22). The total injected dose was calculated by decay correction of the activity present in the animal at 24 h after injection, at which time the clearance of the injected antibodies was considered to be almost negligible, as described earlier (23). The data are presented as the percentage injected dose per gram (%ID/g) of tissue, with the assumption of a tissue density of 1 g/cm^3.

After the scan on day 6, the animals were sacrificed and dissected to confirm the noninvasive small-animal PET data. The radioactivity in dissected tissues was counted in a well-type γ-counter. All data were corrected for physical decay and compared with known standards. Tissue radioactivity was expressed as %ID/g and as a ratio of tumor to normal tissue (T/NT ratio).

Comparative Biodistribution Study of ^{89}Zr-Trastuzumab and ^{111}In-Trastuzumab

Once the minimal required trastuzumab dose had been determined in the protein dose escalation study, a comparative biodistribution study was performed. The aims of this study were to validate HER2/*neu*-specific tumor uptake and to compare the tumor accumulation and organ biodistribution of ^{89}Zr-trastuzumab with those of ^{111}In-trastuzumab. Mice bearing SKOV3 ($n = 5$) or GLC4 ($n = 4$) xenografts were coinjected with 1:1 ^{89}Zr-trastuzumab and ^{111}In-trastuzumab (100 μg of trastuzumab, 1 MBq each). The animals were sacrificed and dissected at days 1, 3, and 6, and the radioactivity in tissues was determined and expressed as %ID/g and as T/NT ratios.

Immunohistochemistry

Xenograft HER2/*neu* expression was confirmed by immunohistochemistry. Formalin-fixed, paraffin-embedded tumors were stained with antibodies against HER2/*neu* (HercepTest; DAKO). Immunohistochemical results were scored semiquantitatively in accordance with the guidelines developed by the American Society of Clinical Oncology and the College of American Pathologists for clinical testing. In short, a 4-tier system was used: 0 corresponded to no staining; 1+ corresponded to weak and incomplete staining; 2+ corresponded to weak to moderate complete staining; and 3+ corresponded to strong, complete circumferential, membranous staining (24). The slides were scored by a pathologist.

Statistical Analysis

Data are presented as mean ± SEM. Statistical analysis was performed with the nonparametric Mann–Whitney test (SPSS version 14.0; SPSS Inc.). *P* values of less than 0.05 were considered significant. The agreement between the quantified in vivo small-animal PET images and the ex vivo biodistribution data was estimated by Bland–Altman analysis (25).

RESULTS

Trastuzumab Conjugation, Radiolabeling, and Quality Control

Trastuzumab was premodified with either *N*-SucDf or *p*-SCN-Bn-DTPA. The number of chelating groups per antibody was estimated to be 1.3 for *N*-SucDf and 1.9 for *p*-SCN-Bn-DTPA. The radiolabeling efficiency for ^{89}Zr-trastuzumab was 77.6% ± 3.9% ($n = 3$), and the radiochemical purity after ultrafiltration was 98.1% ± 1.1% ($n = 3$). The radiolabeling efficiency for ^{111}In-trastuzumab was 89.3% ± 2.1% ($n = 3$), and the radiochemical purity was 97% ± 1% ($n = 3$). The obtained specific activities

were 67.2 ± 2.4 MBq/mg ($n = 3$) for [89]Zr-trastuzumab and 78.2 ± 3.1 MBq/mg ($n = 3$) for ^{111}In-trastuzumab. SE-HPLC analysis (column recovery, $>95\%$; data not shown) of both radiopharmaceuticals revealed no aggregates, fragments, or radioactive impurities. [89]Zr-trastuzumab and ^{111}In-trastuzumab proved to be sterile and endotoxin free.

Immunoreactive Fraction

Flow cytometry confirmed a high level of HER2/*neu* expression for SKOV3 (760 ± 59 events) and a low level of receptor expression for GLC4 (38 ± 1 events). The maintenance of the in vitro binding characteristics of [89]Zr-trastuzumab and ^{111}In-trastuzumab was determined with the cell-binding assay described by Lindmo et al. (*20*). The immunoreactive fraction of [89]Zr-trastuzumab was 0.87 ± 0.06, and that of ^{111}In-trastuzumab was 0.85 ± 0.11. Nonspecific cellular binding was less than 0.10 and was comparable to the binding of the radiopharmaceutical to GLC4.

Stability Testing of Radiolabeled Compounds

[89]Zr-trastuzumab appeared to be stable, with mean decreases in radiochemical purity of only $0.07\% \pm 0.03\%$ in solvent at 4°C and $0.39\% \pm 0.02\%$ in human serum at 37°C per day. The immunoreactive fraction was determined directly after labeling and decreased only marginally with storage in solvent at 4°C (from 0.87 to 0.85 ± 0.06) and in human serum at 37°C (from 0.87 to 0.78 ± 0.01) for up to 7 d.

[111]In-trastuzumab also appeared to be stable, with minimal decreases in protein-bound radioactivity of $0.09\% \pm 0.14\%$ in solvent at 4°C and $0.39\% \pm 0.53\%$ in human serum at 37°C per day. The immunoreactive fraction decreased only slightly with storage in solvent at 4°C (from 0.85 to 0.75 ± 0.04) and in human serum at 37°C (from 0.85 to 0.78 ± 0.08) after 7 d.

In Vivo Biodistribution Studies

In the protein dose escalation study, small-animal PET imaging revealed excellent tumor uptake in all 15 mice. Tumor uptake could already be demonstrated as early as 6 h after [89]Zr-trastuzumab injection, although blood-pool activity was dominant at this time point (Fig. 1A). From day 1 to day 6, tumor uptake significantly increased, whereas blood-pool activity decreased (Fig. 1B). Interestingly, HER2/*neu*-positive metastases, which could be detected easily (Fig. 1C), spontaneously developed in one mouse, even though some metastases were as small as the spatial resolution of the small-animal PET camera (as confirmed by dissection of the animal and pathology). Ex vivo biodistribution data from the protein dose escalation study revealed high tumor uptake (30–33 %ID/g) (Fig. 2) and excellent tumor-to-blood (T/B) and T/NT ratios 6 d after injection. The maximal T/B ratio for animals that received 100 μg of protein was 7.6. Only the liver and the spleen showed slightly higher radioactivity uptake than other organs with a large blood supply; the maximal uptake in the liver and the spleen was 9 %ID/g. The accumulation of radio-
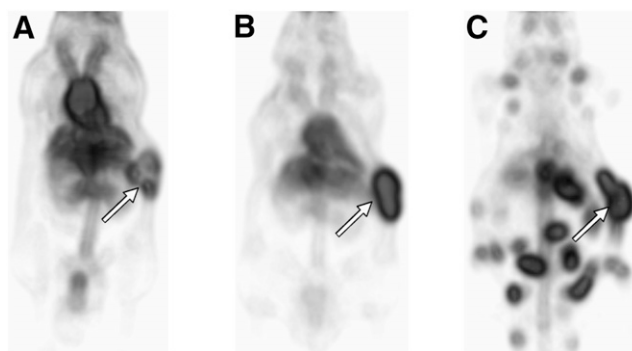

FIGURE 1. Examples of noninvasive small-animal PET images (dorsal presentation). [89]Zr-trastuzumab (5 MBq per mouse) uptake in human SKOV-3 xenografts in 3 mice at 6 h (A), day 1 (B), and day 6 (C, metastasized tumor) after injection is shown. Primary tumors are indicated by arrows.

activity in the muscle and the brain was negligible (<1 %ID/g), resulting in high T/NT ratios.

As shown in Figure 2, there appeared to be a statistically significant difference in radioactivity uptake in the blood and several tissues with a large blood supply (including the heart, kidneys, pancreas, spleen, and muscle). Tumor uptake was not significantly different at the 3 trastuzumab doses ($P = 0.75$). The T/B ratios decreased with increasing doses of trastuzumab (7.3, 5.3, and 4.7, respectively) but did not differ significantly at the 3 applied doses ($P \geq 0.47$). The tumor-to-liver (T/L) ratios varied slightly but not significantly at the 3 doses (being 3.3, 4.6, and 4.0, respectively; $P \geq 0.18$).

Overall, of the tested protein doses, the minimal dose of 100 μg of trastuzumab per animal (approximately 4 mg/kg) was considered to be optimal for imaging because it resulted in excellent tumor uptake and the highest T/B ratios and was therefore used in the comparative biodistribution study of ^{111}In-trastuzumab and [89]Zr-trastuzumab.
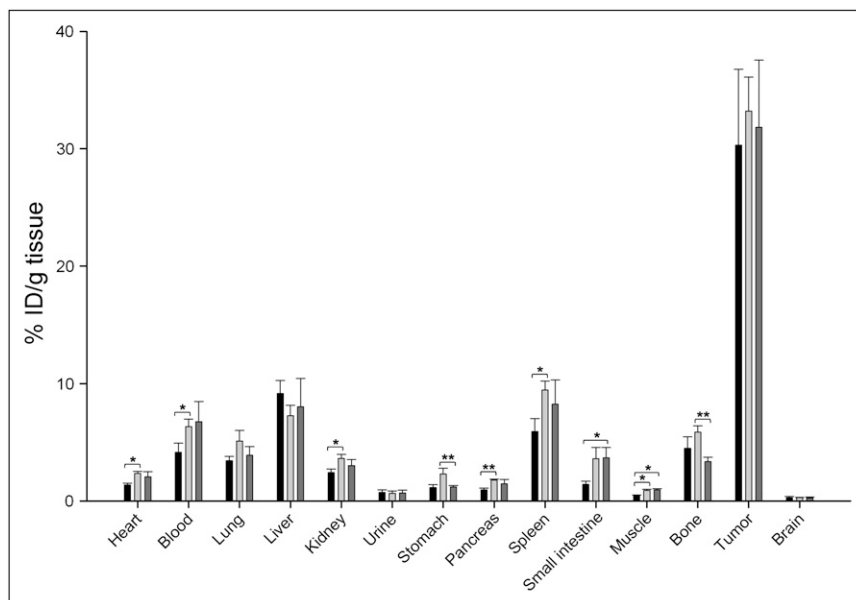
No apoptosis was noted during microscopic evaluation of the tumor tissue at a protein dose of 100–500 μg.

According to the Bland–Altman analysis, all data were well within the limits of agreement and evenly distributed along the mean difference, indicating similarities between the in vivo quantified small-animal PET data and the ex vivo biodistribution data.

The comparative biodistribution study data for [89]Zr-trastuzumab and ^{111}In-trastuzumab in HER2/*neu*-positive SKOV3 tumor–bearing mice and HER2/*neu*-negative GLC4 tumor–bearing mice are shown in Figure 3. For clarity, only days 1 and 6 and the key organs are shown.

The biodistribution data revealed significantly higher uptake of radioactivity in the HER2/*neu*-positive tumor than in the HER2/*neu*-negative tumor. Uptake in the HER2/*neu*-positive tumor could already be demonstrated at day 1 and proved to be similar for [89]Zr-trastuzumab and ^{111}In-trastuzumab (19.3 ± 2.0 %ID/g for [89]Zr-trastuzumab and 17.7 ± 1.9 %ID/g for ^{111}In-trastuzumab; $P = 0.47$). The tumor uptake increased even further to day 6 (33.4 ± 7.6

FIGURE 2. Ex vivo tissue uptake of 100 (black), 250 (light gray), or 500 (dark gray) μg of protein 6 d after intravenous injection of 5 MBq of ^{89}Zr-trastuzumab. Data are presented as %ID/g of tissue (mean ± SEM for 5 mice per group). Significance is indicated (*$P < 0.05$; **$P < 0.01$).

%ID/g for ^{89}Zr-trastuzumab and 39.3 ± 9.5 %ID/g for ^{111}In-trastuzumab; $P = 0.47$). In contrast, the uptake of radioactivity in the HER2/*neu*-negative tumor was lower. At day 1, ^{89}Zr-trastuzumab had accumulated to 15.7 ± 1.3 %ID/g in the HER2/*neu*-negative tumor, and ^{111}In-trastuzumab had accumulated to 15.0 ± 1.4 %ID/g; there was no significant difference between ^{89}Zr-trastuzumab tumor uptake and ^{111}In-trastuzumab tumor uptake ($P = 0.56$). At day 6, the accumulation had decreased to 7.1 ± 0.7 %ID/g for ^{89}Zr-trastuzumab and 6.8 ± 0.8 %ID/g for ^{111}In-trastuzumab ($P = 0.56$).

At day 1, however, there was already a significant difference in tumor uptake in the HER2/*neu*-positive tumor and the HER2/*neu*-negative tumor ($P = 0.027$ for ^{89}Zr-trastuzumab and $P = 0.049$ for ^{111}In-trastuzumab). At day 6, the radiopharmaceutical uptake in the HER2/*neu*-negative tumor was significantly lower than that in the HER2/*neu*-positive tumor ($P = 0.014$ for both ^{89}Zr-trastuzumab and ^{111}In-trastuzumab).

Meanwhile, the percentage of radiolabeled trastuzumab circulating in the blood in mice with HER2/*neu*-positive tumors declined from 20.4 %ID/g for ^{89}Zr-trastuzumab and 18.6 %ID/g for ^{111}In-trastuzumab at day 1 to 4.3 and 5.3 %ID/g, respectively, at day 6. Because of the high tumor uptake and low tissue uptake, excellent T/B and T/NT ratios were achieved at day 6. Liver uptake was limited, and T/L ratios for both radiopharmaceuticals (5.2 for ^{89}Zr-trastuzumab and 7.3 for ^{111}In-trastuzumab) were high and comparable to the data from the protein dose escalation study.

The data obtained in the comparative biodistribution study of ^{89}Zr-trastuzumab and ^{111}In-trastuzumab confirmed the data from the noninvasive small-animal PET images and were similar to the data from the protein dose escalation study at day 6.

Overall, there was no significant difference in uptake. In contrast, there was a good correlation ($R^2 = 0.972$) between ^{89}Zr-trastuzumab uptake and ^{111}In-trastuzumab uptake in tumors (Fig. 4).

Immunohistochemistry

Immunohistochemistry confirmed a high (3+) level of HER2/*neu* expression for the HER2/*neu*-positive SKOV3 tumor and a low (0–1+) level of receptor expression for the HER2/*neu*-negative GLC4 tumor (data not shown).

DISCUSSION

The present study showed that ^{89}Zr-trastuzumab could be radiolabeled efficiently, with preservation of the antigen-binding capacity, and was stable for up to 7 d. A high level of HER2/*neu*-driven tumor uptake of radiolabeled trastuzumab at excellent T/NT ratios was observed. ^{89}Zr-trastuzumab showed a biodistribution similar to that of the control, ^{111}In-trastuzumab, at a spatial resolution unapproachable by SPECT. Produced according to GMP requirements, this radiopharmaceutical is applicable for clinical use.

The tumor uptake of ^{89}Zr-trastuzumab at 100 μg was similar to that at 500 μg, but the T/L ratio at 100 μg was lower than that at 500 μg. This result may have been attributable to faster blood clearance, as animal studies have shown the rapid clearance of human IgG in nude mice with low endogenous IgG titers (*26*)—a phenomenon restricted to the nude-mouse model. The species-specific IgG pharmacokinetics hamper the prediction of the trastuzumab dose required for optimal imaging in humans. Phenomena such as differences in IgG clearance and metabolism, shedding of HER2/*neu*, and tumor load will influence pharmacokinetics in humans and imaging char-
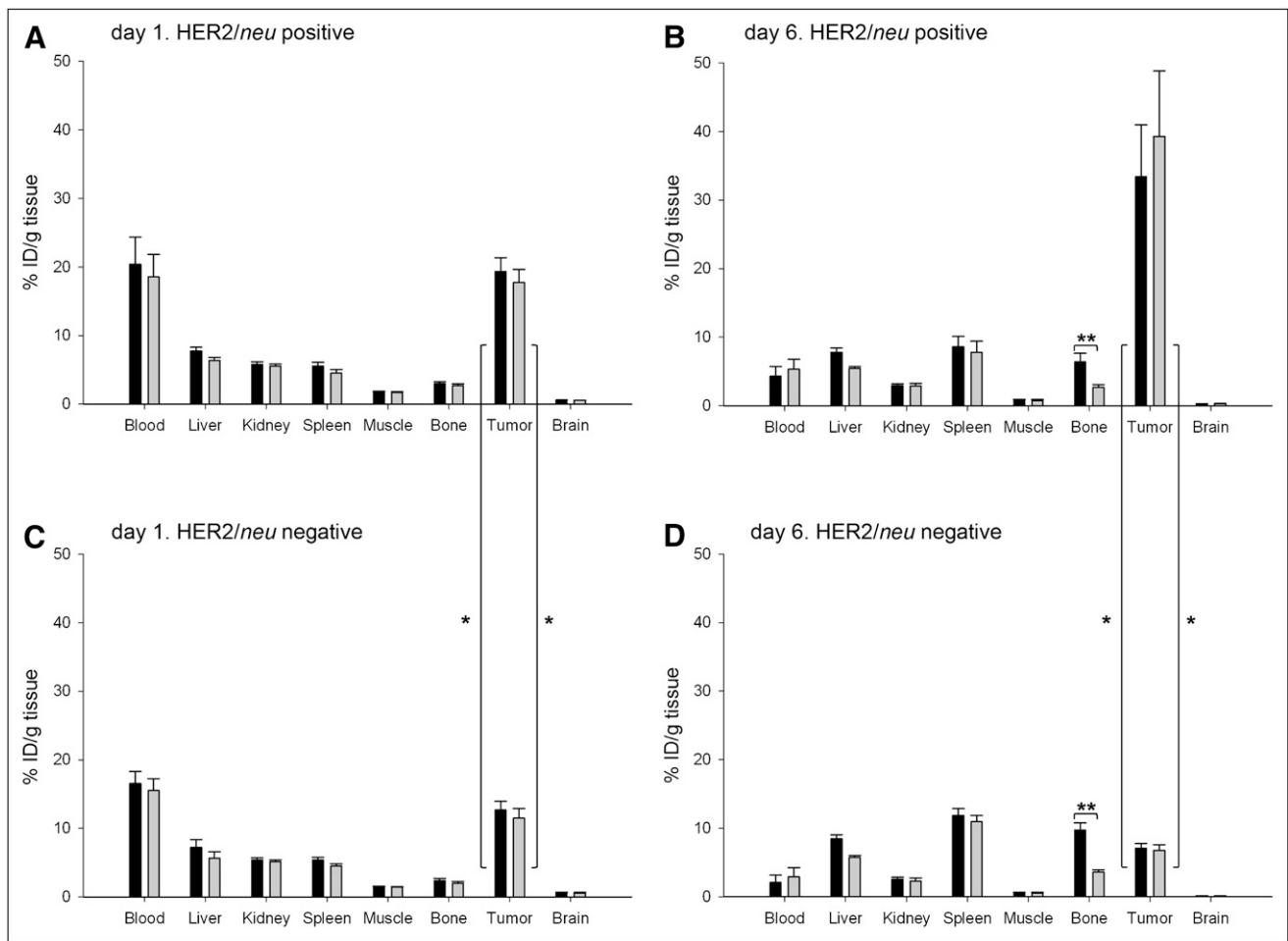
FIGURE 3. Ex vivo tissue uptake after intravenous coinjection of [89]Zr-trastuzumab (black) and ^{111}In-trastuzumab (gray) (100 μg of trastuzumab, 2 MBq in total) at day 1 (A and C) and day 6 (B and D). Data are presented as %ID/g of tissue (mean ± SEM for 5 HER2/*neu*-positive mice and for 4 HER2/*neu*-negative mice per group). Significance is indicated (*$P < 0.05$; **$P < 0.01$).

acteristics. A dose escalation study in patients is therefore mandatory.

Compared with other radiopharmaceuticals developed for HER2/*neu* immunoPET, [124]I-ICR12 demonstrated reasonable and specific uptake (12 %ID/g at 120 h) in athymic mice bearing human HER2/*neu*–overexpressing breast carcinoma xenografts (27). Tumor uptake of ICR12 was further increased, to 20 %ID/g, with residualizing isotopes (28,29). Similar to what we observed in the present study, tumor uptake of ICR12 was not influenced by the protein dose, but the T/B ratio decreased with an increasing amount of protein (30). With the murine predecessor of trastuzumab (4D5), maximal tumor uptake was 35% (31,32), comparable to what we found.

[89]Zr is a relatively new, yet promising, long-lived PET isotope. [89]Zr was considered to be a suitable isotope because it has a sufficiently long physical half-life (3.3 d) to match the relatively slow pharmacokinetics of an intact antibody, is well suited to being combined with an internalizing antibody, and can be used clinically (33). Perk et al. (34) showed that [89]Zr-radiolabeled anti–epidermal growth

factor receptor antibody cetuximab could accurately predict ^{177}Lu and [88]Y (as a substitute for ^{90}Y) biodistributions. [89]Zr-cetuximab therefore has the potential to be used as a scouting procedure in preparation for radioimmunotherapy, for confirming tumor targeting, and for estimating radiation dose delivery to both tumor and normal tissues (34). Using [89]Zr-radiolabeled bevacizumab (an anti–vascular endothelial growth factor mAb), our group reported specific, vascular endothelial growth factor–related tumor uptake at 7 d after injection in a preclinical study (23).

In the first clinical study with a [89]Zr-radiolabeled mAb ([89]Zr-U36, a CD44v6 domain–binding chimeric IgG) immunoPET performed at least as well as CT or MRI for the detection of lymph node metastases in patients with squamous cell carcinoma of the head and neck (35). [89]Zr-oxalate produced according to GMP has been commercially available since the end of 2008.

Clinical HER2/*neu* immunoscintigraphy has been performed with ^{99m}Tc-ICR12, ^{111}In-trastuzumab, and [89]Zr-trastuzumab. In the early 1990s, the rat antibody ^{99m}Tc-ICR12 was administered to 8 breast cancer patients.
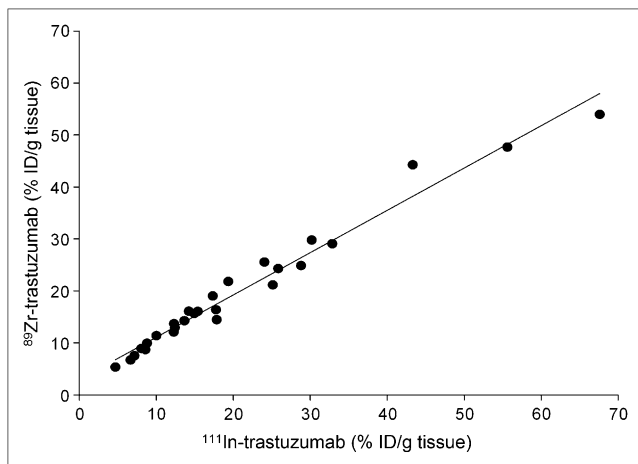
FIGURE 4. Overall correlation of ex vivo tumor uptake of ^{89}Zr and ^{111}In after intravenous coinjection of ^{89}Zr-trastuzumab and ^{111}In-trastuzumab (100 μg of trastuzumab, 2 MBq in total) at days 1, 3, and 6. Correlation coefficient (R^2) was 0.972.

Tomographic images were obtained at 24 h. The study indicated that ^{99m}Tc-ICR12 could be used for the imaging of HER2/*neu* overexpression (*29*), but no further clinical results with this rodent antibody have been published. In a preliminary report, Behr et al. suggested that ^{111}In-trastuzumab could predict the therapeutic efficacy of trastuzumab in 20 patients with HER2/*neu*-overexpressing metastatic breast cancer (*36*). In a study of HER2-positive metastatic breast cancer patients, our group reported that ^{111}In-trastuzumab scintigraphy revealed new tumor lesions in 13 of 15 patients and was therefore suggested to be of value for the clinical staging of HER2/*neu*-positive metastatic breast cancer (*15*). Unfortunately, no clinical studies of HER2/*neu* targeting of smaller proteins have been published.

HER2/*neu* immunoscintigraphy has many potential clinical applications (*33*), including improved diagnosis, guidance for targeted therapy (*37,38*), and early drug development. Therefore, larger studies to prove whether this imaging technique can indeed affect clinical practice are of major interest (*12*).

Generally, large intact antibodies penetrate solid tumor tissue more slowly but constantly, ultimately resulting in a higher level of tumor accumulation, whereas small proteins (mAb fragments, minibodies, single-chain variable antibody fragments, diabodies, or affibodies) penetrate tumor tissue more swiftly but show less tumor uptake because of their rapid blood clearance (*12*). With ^{68}Ga-trastuzumab F(ab′)$_2$ fragments, relatively good tumor uptake was obtained (12 %ID/g), and the loss and recovery of HER2/*neu* induced by the HSP90 inhibitor 17-AAG was quantified (*37*). In a follow-up study, a reduction in ^{68}Ga-F(ab′)$_2$-trastuzumab tumor uptake predicted 17-AAG–induced tumor growth inhibition earlier than a reduction in ^{18}F-FDG tumor uptake (*38*). Divalent single-chain variable antibody fragment (scFv) tumor accumulation is limited

to 2–3 %ID/g (T/B ratio, 3–29); diabody and minibody tumor accumulation is approximately 6 %ID/g (T/B ratio, 3–13) (*12*). Affibody experiments have shown promising results. With affibodies, excellent tumor uptake has been demonstrated (4.4−23 %ID/g), especially when the size of the molecule is considered, and high T/B ratios (7–190) have been observed (*12*).

We have chosen to use the radiolabeled approved intact antibody trastuzumab instead of smaller proteins to determine HER2/*neu* expression. The choice of a radiopharmaceutical for HER2/*neu* imaging should depend on the question to be answered. If only receptor expression is relevant for diagnostic purposes, then imaging can be performed with small proteins, allowing patients to be diagnosed in a single day. If evaluation (and response prediction) of trastuzumab therapy are desired, then radiolabeled intact antibodies, which most likely mimic drug behavior more accurately, are preferable.

^{89}Zr-trastuzumab seems to be a valuable addition to the arsenal of radiolabeled intact antibodies that can be used in patients. It has a higher spatial resolution and a better signal-to-noise ratio than ^{111}In-trastuzumab, and data quantification is more straightforward. The preliminary results obtained with ^{89}Zr-trastuzumab immunoPET in HER2-positive breast cancer patients indicated good radiopharmaceutical uptake by the tumor and excellent spatial resolution (*39*).

CONCLUSION

The present study showed that clinical-grade ^{89}Zr-trastuzumab can be manufactured with high stability and maintenance of antigen binding. The first immunoPET radiopharmaceutical displayed excellent tumor accumulation, with high T/NT ratios and a biodistribution similar to that of ^{111}In-trastuzumab (which was previously used successfully in a clinical study of metastatic breast cancer patients) at a significantly higher spatial resolution and with better T/NT ratios. These data validate this radiopharmaceutical for further clinical testing.

REFERENCES

1. Gross ME, Shazer RL, Agus DB. Targeting the HER-kinase axis in cancer. *Semin Oncol.* 2004;31:9–20.
2. Hynes NE, Stern DF. The biology of erbB-2/neu/HER-2 and its role in cancer. *Biochim Biophys Acta.* 1994;1198:165–184.
3. Slamon DJ, Clark GM, Wong SG, Levin WJ, Ullrich A, McGuire WL. Human breast cancer: correlation of relapse and survival with amplification of the HER-2/neu oncogene. *Science.* 1987;235:177–182.
4. Slamon DJ, Godolphin W, Jones LA, et al. Studies of the HER-2/neu proto-oncogene in human breast and ovarian cancer. *Science.* 1989;244:707–712.

5. Berger MS, Locher GW, Saurer S, et al. Correlation of c-erbB-2 gene amplification and protein expression in human breast carcinoma with nodal status and nuclear grading. *Cancer Res.* 1988;48:1238–1243.

6. Press MF, Pike MC, Chazin VR, et al. Her-2/neu expression in node-negative breast cancer: direct tissue quantitation by computerized image analysis and association of overexpression with increased risk of recurrent disease. *Cancer Res.* 1993;53:4960–4970.

7. Ross JS, Fletcher JA. HER-2/neu (c-erb-B2) gene and protein in breast cancer. *Am J Clin Pathol.* 1999;112:S53–S67.

8. Oldenhuis CN, Oosting SF, Gietema JA, de Vries EG. Prognostic versus predictive value of biomarkers in oncology. *Eur J Cancer.* 2008;44:946–953.

9. Hudis CA. Trastuzumab: mechanism of action and use in clinical practice. *N Engl J Med.* 2007;357:39–51.

10. Yaziji H, Goldstein LC, Barry TS, et al. HER-2 testing in breast cancer using parallel tissue-based methods. *JAMA.* 2004;291:1972–1977.

11. McCormick SR, Lillemoe TJ, Beneke J, Schrauth J, Reinartz J. HER2 assessment by immunohistochemical analysis and fluorescence in situ hybridization: comparison of HercepTest and PathVysion commercial assays. *Am J Clin Pathol.* 2002;117:935–943.

12. Dijkers ECF, de Vries EGE, Kosterink JGW, Brouwers AH, Lub-De Hooge MN. Immunoscintigraphy as potential tool in the clinical evaluation of HER2/neu targeted therapy. *Curr Pharm Des.* 2008;14:3348–3362.

13. Lear-Kaul KC, Yoon HR, Kleinschmidt-DeMasters BK, McGavran L, Singh M. Her-2/neu status in breast cancer metastases to the central nervous system. *Arch Pathol Lab Med.* 2003;127:1451–1457.

14. Lub-De Hooge MN, Kosterink JG, Perik PJ, et al. Preclinical characterisation of ^{111}In-DTPA-trastuzumab. *Br J Pharmacol.* 2004;143:99–106.

15. Perik PJ, Lub-De Hooge MN, Gietema JA, et al. Indium-111-labeled trastuzumab scintigraphy in patients with human epidermal growth factor receptor 2-positive metastatic breast cancer. *J Clin Oncol.* 2006;24:2276–2282.

16. Verel I, Visser GW, Boellaard R, Stigter-van Walsum M, Snow GB, van Dongen GA. ^{89}Zr immuno-PET: comprehensive procedures for the production of ^{89}Zr-labeled monoclonal antibodies. *J Nucl Med.* 2003;44:1271–1281.

17. Ruegg CL, Anderson-Berg WT, Brechbiel MW, Mirzadeh S, Gansow OA, Strand M. Improved in vivo stability and tumor targeting of bismuth-labeled antibody. *Cancer Res.* 1990;50:4221–4226.

18. Hnatowich DJ, Childs RL, Lanteigne D, Najafi A. The preparation of DTPA-coupled antibodies radiolabeled with metallic radionuclides: an improved method. *J Immunol Methods.* 1983;65:147–157.

19. van Geelen CM, de Vries EG, Le TK, van Weeghel RP, de Jong S. Differential modulation of the TRAIL receptors and the CD95 receptor in colon carcinoma cell lines. *Br J Cancer.* 2003;89:363–373.

20. Lindmo T, Boven E, Cuttitta F, Fedorko J, Bunn PA Jr. Determination of the immunoreactive fraction of radiolabeled monoclonal antibodies by linear extrapolation to binding at infinite antigen excess. *J Immunol Methods.* 1984;72:77–89.

21. Loening AM, Gambhir SS. AMIDE: a free software tool for multimodality medical image analysis. *Mol Imaging.* 2003;2:131–137.

22. Verel I, Visser GW, Boellaard R, et al. Quantitative ^{89}Zr immuno-PET for in vivo scouting of ^{90}Y-labeled monoclonal antibodies in xenograft-bearing nude mice. *J Nucl Med.* 2003;44:1663–1670.

23. Nagengast WB, de Vries EG, Hospers GA, et al. In vivo VEGF imaging with radiolabeled bevacizumab in a human ovarian tumor xenograft. *J Nucl Med.* 2007;48:1313–1319.

24. Wolff AC, Hammond ME, Schwartz JN, et al. American Society of Clinical Oncology/College of American Pathologists guideline recommendations for human epidermal growth factor receptor 2 testing in breast cancer. *J Clin Oncol.* 2007;25:118–145.

25. Bland JM, Altman DG. Statistical methods for assessing agreement between two methods of clinical measurement. *Lancet.* 1986;1:307–310.

26. Meric-Bernstam F, Mills GB. Mammalian target of rapamycin. *Semin Oncol.* 2004;31:10–17.

27. Bakir MA, Eccles S, Babich JW, et al. c-erbB2 protein overexpression in breast cancer as a target for PET using iodine-124-labeled monoclonal antibodies. *J Nucl Med.* 1992;33:2154–2160.

28. Dean CJ, Eccles SA, Valeri M, et al. Rat MAbs to the product of the c-erbB-2 proto-oncogene for diagnosis and therapy in breast cancer. *Cell Biophys.* 1993;22:111–127.

29. Allan SM, Dean C, Fernando I, et al. Radioimmunolocalisation in breast cancer using the gene product of c-erbB2 as the target antigen. *Br J Cancer.* 1993;67:706–712.

30. Smellie WJ, Dean CJ, Sacks NP, et al. Radioimmunotherapy of breast cancer xenografts with monoclonal antibody ICR12 against c-erbB2 p185: comparison of IodoGen and *N*-succinimidyl 4-methyl-3-(tri-*n*-butylstannyl)benzoate radio-iodination methods. *Cancer Res.* 1995;55(23 suppl):5842s–5846s.

31. Milenic DE, Garmestani K, Brady ED, et al. Targeting of HER2 antigen for the treatment of disseminated peritoneal disease. *Clin Cancer Res.* 2004;10:7834–7841.

32. Tsai SW, Sun Y, Williams LE, Raubitschek AA, Wu AM, Shively JE. Biodistribution and radioimmunotherapy of human breast cancer xenografts with radiometal-labeled DOTA conjugated anti-HER2/neu antibody 4D5. *Bioconjug Chem.* 2000;11:327–334.

33. van Dongen GA, Visser GW, Lub-De Hooge MN, de Vries EG, Perk LR. Immuno-PET: a navigator in monoclonal antibody development and applications. *Oncologist.* 2007;12:1379–1389.

34. Perk LR, Visser GW, Vosjan MJ, et al. ^{89}Zr as a PET surrogate radioisotope for scouting biodistribution of the therapeutic radiometals ^{90}Y and ^{177}Lu in tumor-bearing nude mice after coupling to the internalizing antibody cetuximab. *J Nucl Med.* 2005;46:1898–1906.

35. Borjesson PK, Jauw YW, Boellaard R, et al. Performance of immuno-positron emission tomography with zirconium-89-labeled chimeric monoclonal antibody U36 in the detection of lymph node metastases in head and neck cancer patients. *Clin Cancer Res.* 2006;12:2133–2140.

36. Behr TM, Behe M, Wormann B. Trastuzumab and breast cancer. *N Engl J Med.* 2001;345:995–996.

37. Smith-Jones PM, Solit DB, Akhurst T, Afroze F, Rosen N, Larson SM. Imaging the pharmacodynamics of HER2 degradation in response to Hsp90 inhibitors. *Nat Biotechnol.* 2004;22:701–706.

38. Smith-Jones PM, Solit D, Afroze F, Rosen N, Larson SM. Early tumor response to Hsp90 therapy using HER2 PET: comparison with ^{18}F-FDG PET. *J Nucl Med.* 2006;47:793–796.

39. Dijkers ECF, Lub-De Hooge MN, Kosterink JG, et al. Characterization of ^{89}Zr-trastuzumab for clinical HER2 immunoPET imaging [abstract]. *J Clin Oncol.* 2007;25:3508.